Proc. Natl. Acad. Sci. USA
Vol. 76, No. 1, pp. 56–60, January 1979
Biochemistry

Subnanosecond motions of tryptophan residues in proteins

(protein dynamics/rotational relaxation/fluorescence polarization/emission anisotropy/synchrotron radiation)

IAN MUNRO, ISRAEL PECHT, AND LUBERT STRYER

Department of Structural Biology, Sherman Fairchild Center, Stanford University School of Medicine, Stanford, California 94305

Communicated by Gregorio Weber, August 23, 1978

ABSTRACT **The dynamics of protein molecules in the subnanosecond and nanosecond time range were investigated by time-resolved fluorescence polarization spectroscopy. Synchrotron radiation from a storage ring was used as a pulsed light source to excite the single tryptophan residue in a series of proteins. The full width at half maximum of the detected light pulse was 0.65 nsec, making it feasible to measure emission anisotropy kinetics in the subnanosecond time range and thereby to resolve internal rotational motions. The proteins investigated exhibit different degrees of rotational freedom of their tryptophan residue, ranging from almost no mobility to nearly complete freedom in the subnanosecond time range. The tryptophan residue of *Staphylococcus aureus* nuclease B (20,000 daltons) has a single rotational correlation time (ϕ) of 9.9 nsec at 20°C, corresponding to a rotation of the whole protein molecule. By contrast, bovine basic A1 myelin protein (18,000 daltons) exhibits ϕ of 0.09 and 1.26 nsec, showing that the tryptophan residue in this protein is highly flexible. The single tryptophan of human serum albumin (69,000 daltons) has almost no rotational freedom at 8°C (ϕ = 31.4 nsec), whereas at 43°C it rotates rapidly (ϕ_1 = 0.14 nsec) within a cone of semiangle 26° in addition to rotating together with the whole protein (ϕ_2 = 14 nsec). Of particular interest is the large angular range (semiangle, 34°) and fast rate (ϕ_1 = 0.51 nsec) of the rotational motion of the tryptophan residue in *Pseudomonas aeruginosa* azurin (14,000 daltons). This residue is known to be located in the hydrophobic interior of the protein. The observed amplitudes and rates of these internal motions of tryptophan residues suggest that elementary steps in functionally significant conformational changes may take place in the subnanosecond time range.**

The importance of protein flexibility in catalysis, allosteric regulation, energy transduction, signaling, and other biological processes is becoming increasingly evident (1–4). Some interesting questions now are: What is the range of motions in proteins? On what time scale do they occur? How are some of these motions controlled and coordinated? Experimental and theoretical studies indicate that proteins undergo rapid fluctuations in structure. Lakowicz and Weber (5) measured the effect of oxygen on the fluorescence intensity and excited-state lifetime of tryptophan residues in a series of proteins. They found that all tryptophan residues in the proteins studied were dynamically quenched by oxygen. The accessibility of internal tryptophan residues to quenching by oxygen molecules during their excited-state lifetime showed that proteins undergo structural fluctuations on the nanosecond time scale. The recent theoretical studies by McCammon *et al.* (6) indicated that some of these fluctuations may in fact occur in the picosecond time range. Their simulation of the dynamics of the internal motions of bovine pancreatic trypsin inhibitor showed root mean square atom fluctuations of 0.9 Å in times of picoseconds.

We have carried out time-resolved emission anisotropy studies of the tryptophan fluorescence of a series of proteins to determine the angular range and kinetics of internal rotational motions of this chromophore. Nanosecond emission anisotropy studies have previously provided information concerning the segmental flexibility of domains of immunoglobulins (7, 8) and myosin (9). These studies had a time resolution of several nanoseconds and used extrinsic fluorescent probes. By using synchrotron radiation, we are now able to monitor directly the rotational motions of tryptophan residues in proteins, obviating any perturbations that may be caused by the insertion of an extrinsic probe. The distinctive properties of synchrotron radiation for these studies are its subnanosecond pulse width, high repetition rate and reproducibility, and high intensity in the ultraviolet region (10, 11). Proteins with a single tryptophan residue were studied because the interpretation of their emission anisotropy kinetics is more definitive than for proteins with multiple tryptophans. The molecules investigated were human serum albumin (69,000 daltons) (12), *Staphylococcus aureus* nuclease B (20,000 daltons) (13), human basic A1 myelin protein (18,000 daltons) (14), and *Pseudomonas aeruginosa* holoazurin and apoazurin (14,000 daltons) (15).

The publication costs of this article were defrayed in part by page charge payment. This article must therefore be hereby marked "*advertisement*" in accordance with 18 U. S. C. §1734 solely to indicate this fact.

THEORY AND ANALYSIS

In a time-resolved emission anisotropy experiment, an isotropic sample is excited by a pulse of y-polarized (vertically polarized) light, which produces an ensemble of preferentially aligned excited molecules. The orientations of the excited molecules then become randomized by rotational Brownian motion. For a fluorescent chromophore in a macromolecule, the rate of randomization depends both on the degree of flexibility of this group with respect to the macromolecule and on the size, shape, and internal motions of the macromolecule. These rotational motions can be monitored by measuring $y(t)$ and $x(t)$, the intensities of the y-polarized and x-polarized (horizontally polarized) components of the fluorescence emission as a function of time (for reviews, see refs. 16 and 17). The total fluorescence intensity $F(t)$ and the emission anisotropy $A(t)$ are defined by

$$F(t) = y(t) + 2x(t) \quad [1]$$

$$A(t) = [y(t) - x(t)]/[y(t) + 2x(t)]. \quad [2]$$

The simplest case is a chromophore with a single excited-state lifetime rotating in common with a rigid sphere. $F(t)$ and $A(t)$ are then given by

$$F(t) = F_0 e^{-t/\tau} \quad [3]$$

$$A(t) = A_0 e^{-t/\phi} \quad [4]$$

in which F_0 is the initial fluorescence intensity and τ is the excited state lifetime. For a rigid sphere, the rotational correlation time ϕ is given by

$$\phi = V\eta/(kT) = M(\bar{v} + h)\eta/(kT) \quad [5]$$

in which V is the molecular volume, η is the viscosity of the medium, k is the Boltzmann constant, T is the absolute temperature, M is the molecular weight, $\bar{v}$ is the partial specific volume, and h is the degree of hydration.

The excited state and emission anisotropy kinetics of a chromophore in a macromolecule are likely to be more complex than represented by Eqs. 3 and 4. If the chromophore has more than one kind of environment during the excited-state lifetime, $F(t)$ is given by a sum of exponential terms

$$F(t) = \sum_i f_i e^{-t/\tau_i} \quad [6]$$

in which f_i is the initial intensity of the ith component. If the macromolecule is nonspherical (18) or if there are any modes of flexibility (19), $A(t)$ is given by a sum of exponential terms

$$A(t) = \sum_j a_j e^{-t/\phi_j} \quad [7]$$

in which a_j is the initial emission anisotropy of the jth component. Suppose that the emission transition moment of a fluorescent chromophore attached to a macromolecule rotates freely within a cone of semiangle α. $A(t)$ is then given by

$$A(t) = a_1 e^{-t/\phi_1} + a_2 e^{-t/\phi_2} \quad [8]$$

in which the first term arises from rotation inside the cone and the second, from rotation in common with the macromolecule (19–21). In this expression, ϕ_2 is the rotational correlation time of the macromolecule, and ϕ_1 depends both on the diffusion constant within the cone and on its angular range. The semiangle α of this cone is related to these coefficients by

$$a_2/(a_1 + a_2) = a_2/A_0 = \cos^2\alpha(1 + \cos\alpha)^2/4. \quad [9]$$

For isotropic rotations, the rotational diffusion coefficient R (rad^2 sec^{-1}) is equal to $1/6\phi$. For diffusion within a cone of semiangle α (G. Weber, personal communication),

$$R = (1/6\phi_1)[\alpha^2/(\pi/2)^2]. \quad [10]$$

The preceding equations for $F(t)$ and $A(t)$ assume that the light pulse as measured by the detection system is a δ function. However, the actual light pulse has a finite duration, and so the experimentally observed quantities $y_e(t)$ and $x_e(t)$ are convolutions of $y(t)$ and $x(t)$ with the light pulse. These convolutions were taken into account in deriving amplitudes, excited-state lifetimes, and ϕ values from $y_e(t)$ and $x_e(t)$. We used a nonlinear least squares fit procedure (22–25) to analyze excited-state decay data and extended this method to analyze emission anisotropy kinetics.

MATERIALS AND METHODS

Synchrotron Radiation Source and Fluorescence Detection System. Synchrotron radiation from the Stanford positron-electron accelerator ring (SPEAR) was used as the pulsed light source (1.28 MHz) in these studies (26). A collimating lens, 45° mirror, and focusing lens brought the beam into a Heath f/6.8 Czerny–Turner monochromator. The bandwidth was 4 nm or less in our emission anisotropy experiments. The excitation beam was passed through a Glan–Thomson prism polarizer and focused by a silica (Dynasil 1000) lens to a 0.2-mm-diameter spot in a 1 × 1 cm thermostatted quartz cuvet. The emission viewed at 90° was passed through 1.0 M $CuSO_4$ (1-cm path) to reject scattered light, collected by a silica lens, and transmitted through an ultraviolet sheet polarizer (3M type 105UVWRMR) onto a RCA 8850 photomultiplier tube.

The emission kinetics were measured with a single-photon counting apparatus (7, 16). The start pulse into the time-to-amplitude converter (Ortec model 457) came from the anode of the photomultiplier (operated at 2950 V) after it was amplified by a Hewlett–Packard preamplifier (22 db, type 10855A) and shaped by an Ortec constant fraction discriminator (model 473A). The stop pulse, also shaped by a constant fraction discriminator, came from a Philips 56 AVP photomultiplier (operated in the multiphoton mode at 2600 V) which monitored about 10% of the incident light (through a Corning 7-60 filter) before it entered the monochromator. A Hewlett–Packard multichannel pulse height analyzer (model 5421) detected the output of the time-to-amplitude converter. The fluorescence intensity or scattered light intensity was attenuated when necessary to set the photomultiplier count rate below 12 KHz to avoid distortions due to multiphoton events.

Experimental data were collected in the following sequence. First, the instrument response function $L(t)$ was measured by using an aluminum reflector as a light scatterer. The timing and shape of the photomultiplier output depend on wavelength, whereas the temporal characteristics of synchrotron radiation are independent of wavelength (11). Consequently, $L(t)$ was measured by using incident light at the wavelength of maximal fluorescence emission rather than at the excitation wavelength. The sample was then excited with vertically (y) polarized light. Emission anisotropy kinetics were measured by alternating the emission polarizer setting from vertical (y) to horizontal (x) every 20 sec (27). Data were collected for periods ranging from 10 to 40 min to accumulate at least 50,000 counts in the peak channel. The y and x components of a buffer blank were then collected and subtracted from the respective components of the sample fluorescence.

Proteins. Azurin from *P. aeruginosa* with an A_{280}/A_{625} ratio of 2 and apoazurin were prepared as described (28, 29). Nuclease B was isolated from *S. aureus* (13). Human serum albumin, purchased from Sigma, was chromatographed on Sephadex G-150 to remove oligomers. Bovine basic A1 myelin protein was prepared according to the published procedure (30). Nuclease B was dissolved in 0.1 M Tris, pH 8.1/10 mM $CaCl_2$. All other proteins were in 0.15 M NaCl/0.05 M sodium phosphate, pH 7.4. The concentrations of proteins were adjusted to give an absorbance of 0.1 at the excitation wavelength of 300 nm.

RESULTS

The time course of the synchrotron light pulse at 340 nm as detected by the single-photon counting system is shown in Fig. 1*A*. The full width at half maximum was 0.65 nsec. The full widths at 0.1, 0.01, and 0.001 maximum were 1.2, 1.9, and 3.2 nsec, respectively. The number of photons per pulse at the sample cell was 10^4 at 340 nm for a 4-nm bandpass and a circulating electron current of 10 mA. The effect of the finite duration of this detected light pulse on the emission anisotropy kinetics is shown in the simulations of Fig. 1*B*, which were calculated by convolving the light pulse with an excited-state lifetime of 5.0 nsec, an A_0 of 0.2, and a series of ϕ values ranging from 0.1 to 10 nsec. The initial portions of these plots of the logarithm of the emission anisotropy versus time exhibit curvature because more molecules with a high emission anisotropy are excited than decay during the light pulse. The slopes of subsequent portions of these plots are inversely proportional to ϕ except for ϕ values that are less than the width of the light pulse. These calculations show that ϕ as short as 100 psec can be measured with this light pulse and detection system.

The emission anisotropy kinetics of *N*-acetyltryptophanamide in glycerol/water mixtures (Fig. 1*C*) were measured to test the detection system and to obtain ϕ values for the tryptophan chromophore in isotropic media of known viscosity. An excitation wavelength of 300 nm was chosen to obtain a high initial emission anisotropy (31). Also, tryptophan residues in proteins can be excited at this wavelength without exciting tyrosines (32). The observed ϕ values were 16.8, 3.7, 0.38, and

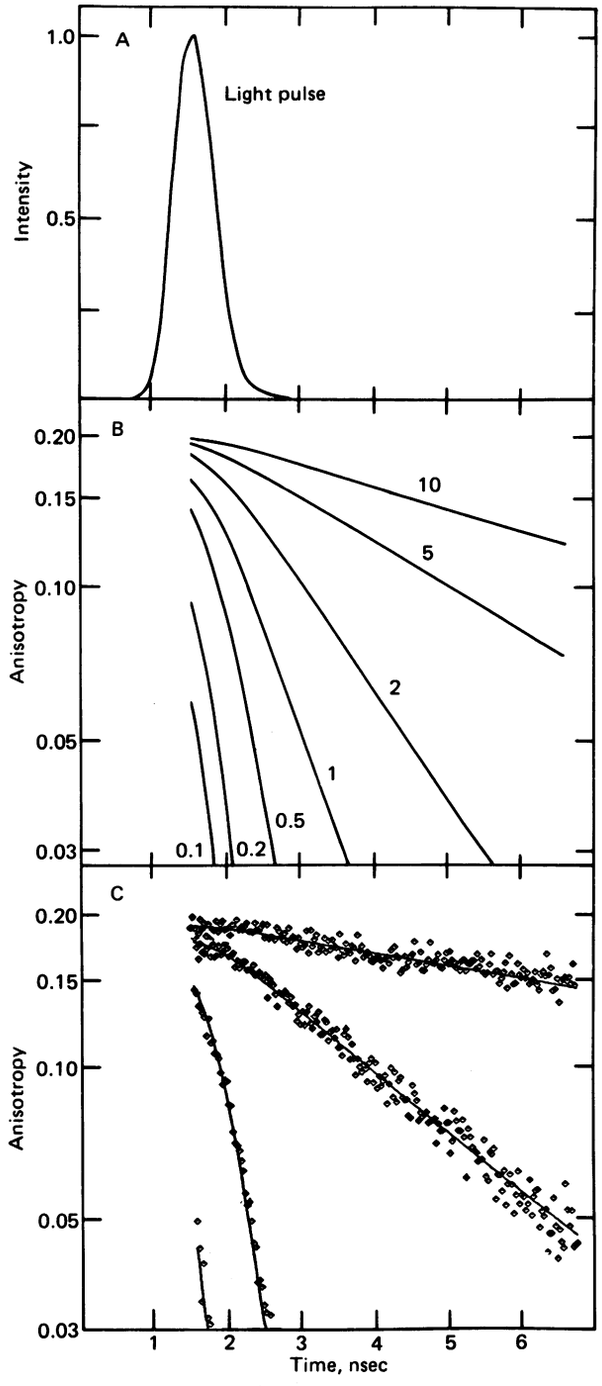

FIG. 1. (*A*) Time course of the synchrotron light pulse at 340 nm detected by an RCA 8850 photomultiplier tube and a single-photon counting apparatus. The full width at half maximum is 0.65 nsec. (*B*) Simulated emission anisotropy kinetics for ϕ = 0.1, 0.2, 0.5, 1, 2, 5, and 10 nsec for A_0 = 0.2 and τ = 5.0 nsec. The light pulse shown in *A* was used in the convolution. (*C*) Emission anisotropy kinetics of 10 μM *N*-acetyltryptophanamide in glycerol/water mixtures at 20°C excited at 300 nm. The observed ϕ values (mean ± SD) are 16.8 ± 0.3 nsec in pure glycerol (top curve), 3.7 ± 0.1 nsec in 92% (wt/wt) glycerol, 0.38 ± 0.10 nsec in 66% glycerol, and <0.05 nsec in 12% glycerol. The excited-state lifetimes are 5.8, 5.3, 5.1, and 3.9 nsec, respectively.

<0.05 nsec in glycerol/water mixtures having viscosities of 1445, 304, 17, and 1.4 cp, respectively, at 20°C.

The emission anisotropy kinetics of nuclease B and myelin basic protein (Fig. 2) illustrate the range of rotational freedom in proteins. The tryptophan residue in nuclease B undergoes a single mode of rotational motion, with A_0 = 0.177 and ϕ = 9.85 nsec. This rotational correlation time is comparable to the value of 7.6 nsec calculated from Eq. **5** for a 20,000-dalton rigid hydrated sphere at 20°C, assuming $\bar{v}$ = 0.73 cm^3/g and h = 0.2 cm^3/g. Thus, the tryptophan residue in nuclease B has little internal rotational freedom. By contrast, the tryptophan chromophore in myelin basic protein undergoes very rapid rotational relaxation. The observed ϕ values of 0.09 and 1.26 nsec are much shorter than the 6.9 nsec calculated for an 18,000-dalton rigid hydrated sphere at 20°C. The absence of any long rotational component in the observed anisotropy kinetics indicates that the tryptophan residue in myelin basic protein has a very high degree of rotational freedom.

The effect of temperature on the emission anisotropy kinetics of human serum albumin is shown in Fig. 3. At 8°C, the tryptophan in this protein exhibits essentially one kind of rotational motion, with A_0 = 0.19 and ϕ = 31.4 nsec. This ϕ is comparable to the value of 39.9 nsec calculated for a rigid hydrated sphere, indicating that it arises from a rotation of tryptophan together with the whole protein or a large domain of it. At 43°C, this tryptophan residue acquires rotational freedom independent of the whole protein, as reflected in the rapid component with a_1 = 0.064 and ϕ_1 = 0.14 nsec, which was essentially absent at 8°C. The long component has a_1 = 0.17 and ϕ_2 = 14 nsec. The amplitude of the 0.14-nsec component indicates that it could arise from a very rapid rotation of the tryptophan residue within a cone of semiangle 26°, as calculated from Eq. **10**.

Two distinct kinds of rotational motions are also evident in the emission anisotropy kinetics of holoazurin (Fig. 4). The tryptophan residue in this protein exhibits both a very rapid rotation (a_1 = 0.101 and ϕ_1 = 0.51 nsec) and a slower rotation (a_2 = 0.132 and ϕ_2 = 11.8 nsec). The observed ϕ_2 can be attributed to a rotation of tryptophan together with the whole molecule because it is larger than the ϕ of 8.5 nsec calculated for a 14,000-dalton rigid hydrated sphere at 8°C. The amplitude of the 0.51-nsec rotational component can be interpreted to indicate that the tryptophan residue in holoazurin rotates

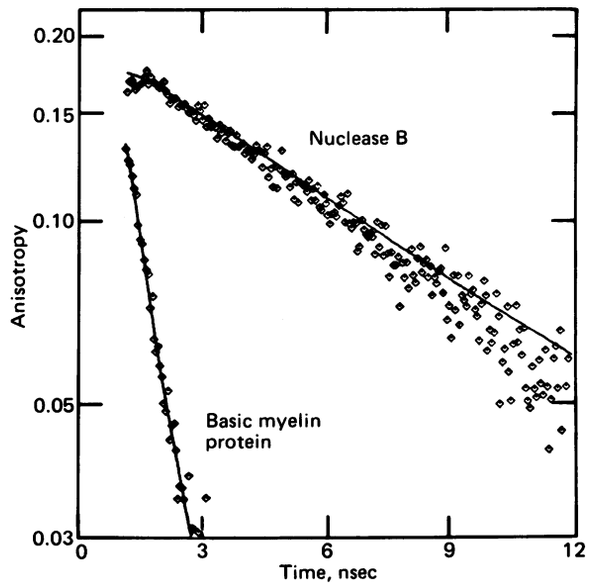

FIG. 2. Comparison of the emission anisotropy kinetics of *S. aureus* nuclease B with those of myelin basic protein. The best-fit parameters for nuclease B (20°C, excited at 300 nm) are τ = 5.05 nsec, A_0 = 0.177 ± 0.001, and ϕ = 9.85 ± 0.17 nsec. For basic myelin protein (20°C, excited at 300 nm), f_1 = 0.69, τ_1 = 1.97 nsec, f_2 = 0.31, τ_2 = 4.7 nsec, a_1 = 0.15 ± 0.006, ϕ_1 = 0.09 ± 0.004 nsec, a_2 = 0.106 ± 0.001, and ϕ_2 = 1.26 ± 0.02 nsec.

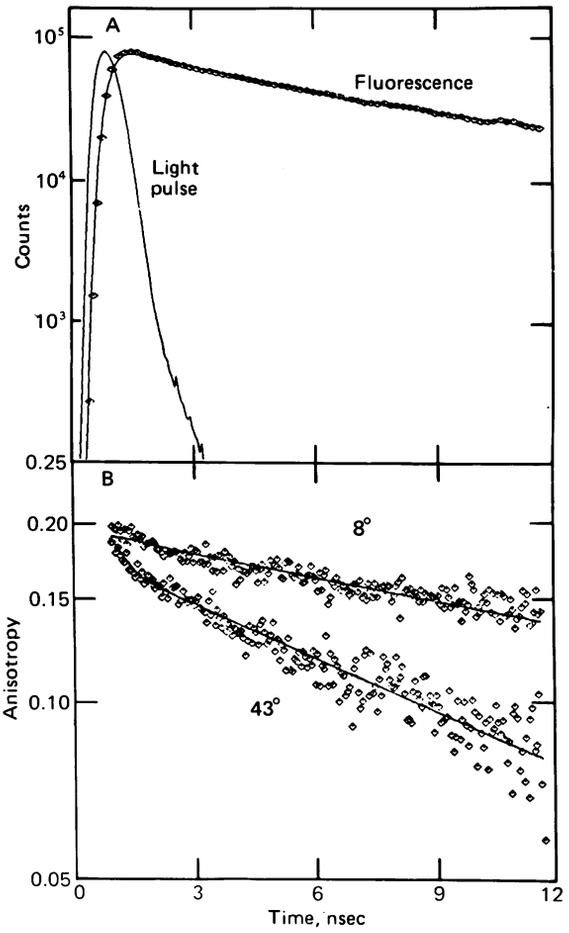

FIG. 3. (*A*) Emission kinetics of human serum albumin at 8°C excited at 300 nm. The observed fluorescence kinetics fit the convolution of the light pulse with a two-component decay in which f_1 = 0.039, τ_1 = 2.78 nsec, f_2 = 0.61, and τ_2 = 9.37 nsec. (*B*) Emission anisotropy kinetics of human serum albumin at 8°C and 43°C. The observed anisotropy kinetics at 8°C fit the curve calculated for a_1 = 0.003 ± 0.001, ϕ_1 = 0.76 ± 0.4 nsec, a_2 = 0.19 ± 0.0002, and ϕ_2 = 31.4 ± 0.3 nsec. At 43°C, a_1 = 0.064 ± 0.03, ϕ_1 = 0.14 ± 0.1 nsec, a_2 = 0.17 ± 0.002, and ϕ_2 = 14 ± 0.6 nsec.

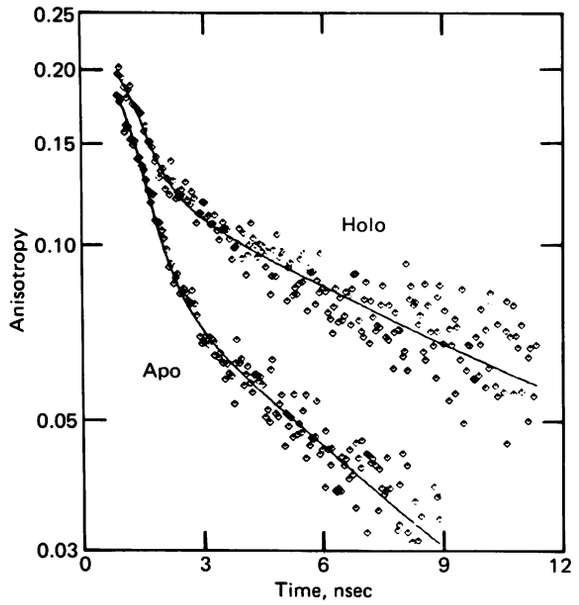

FIG. 4. Comparison of the emission anisotropy kinetics of the holoprotein (HOLO) and apoprotein (APO) forms of *P. aeruginosa* azurin (8°C, excited at 300 nm). The best-fit parameters for the holoprotein are f_1 = 0.50, τ_1 = 0.75 nsec, f_2 = 0.50, τ_2 = 4.15 nsec, a_1 = 0.101 ± 0.002, ϕ_1 = 0.51 ± 0.02 nsec, a_2 = 0.132 ± 0.0008, and ϕ_2 = 11.8 ± 0.3 nsec. For the apoprotein, f_1 = 0.40, τ_1 = 0.88 nsec, f_2 = 0.60, τ_2 = 4.79 nsec, a_1 = 0.139 ± 0.002, ϕ_1 = 0.49 ± 0.01 nsec, a_2 = 0.092 ± 0.0006, and ϕ_2 = 6.84 ± 0.12 nsec.

very rapidly within a cone of semiangle 34°. The emission anisotropy curve for apoazurin lies below that of holoazurin, showing that the removal of the active site copper ion increases the flexibility of the molecule. The angular range of the very rapid rotational motion of tryptophan is larger in apoazurin (44°) than in holoazurin. Furthermore, the ϕ_2 of 5.8 nsec observed for apoazurin is significantly less than the value, 8.5 nsec, calculated for a rigid hydrated sphere.

DISCUSSION

The use of synchrotron radiation as a pulsed light source enabled us to measure the emission anisotropy kinetics of the single tryptophan residue in a series of proteins and thereby monitor the rotational motions of this chromophore. Tunable mode-locked lasers with pulse widths of less than 50 psec and high repetition rates, which are now becoming available (33), will complement synchrotron radiation in the study of these very rapid processes. We found that tryptophan is nearly immobile in some proteins whereas it has a high degree of subnanosecond rotational mobility in others. The virtual absence of rotational freedom of the tryptophan residue in nuclease B is consistent with the x-ray crystallographic finding that the tryptophan of nuclease A is hydrogen-bonded and in close contact with the carboxy-terminal helix (34). By contrast, the tryptophan residue in myelin basic protein has ϕ values that are much shorter than the value calculated for a rigid macromolecule. This finding of a very high degree of rotational freedom agrees with hydrodynamic, circular dichroism, and low-angle x-ray scattering studies (35–37) showing that myelin basic protein behaves as a random coil. The tryptophan residue in holoazurin exhibits two distinct modes of rotational freedom. The amplitude of the very rapid component (ϕ_1 = 0.51 nsec) can be interpreted in terms of a free rotation of the tryptophan chromophore within a cone of semiangle 34°. This large angular range is striking because tryptophan is known to be located in the interior of azurin. The tryptophan fluorescence of nearly all proteins studied thus far consists of a structureless band with a peak between about 325 and 355 nm (31). By contrast, the tryptophan residue in azurin exhibits a fluorescence spectrum with vibrational fine structure peaking at 308 nm, indicating that it is in a highly hydrophobic milieu (38). Furthermore, recent x-ray crystallographic studies of azurin show that its tryptophan residue is surrounded by nonpolar side chains in the interior of the molecule and that it is not hydrogen-bonded (39).

The significance of these experiments is twofold. First, the range of observable rates of rotational motion has been extended by two orders of magnitude. Nuclear magnetic resonance spectroscopy previously provided information about rotational motions of aromatic groups in proteins occurring in times of 10^{-8} to 1 sec (40–44). Second, we have found that the tryptophan residue of some proteins is in fact mobile over a large angle in the subnanosecond time range. Our emission anisotropy studies of azurin demonstrate that a protein can have an interior that is fluid-like in the subnanosecond time range, as suggested by theoretical calculations (6). However, it must be stressed that fluidity on this time scale is not characteristic of all proteins, as shown by the relatively rigid environment of tryptophan in nuclease B and human serum albumin. It will be interesting to relate subnanosecond motions in proteins to biological activities

such as catalysis and transport. Subnanosecond structural fluctuations may be the elementary steps in conformational transitions that are essential for these processes.

We thank William Carlsen and Sandra Slaughter for their invaluable help. Dr. Drew Ridge, Dr. Robert L. Baldwin, and Dr. Dvora Teitelbaum kindly provided samples of proteins. This work was supported by grants from the National Institute of General Medical Sciences (GM 24032 and GM 17367). The time-resolved fluorescence studies were carried out at the Stanford Synchrotron Radiation Laboratory, which is supported by the National Science Foundation (DMR 77-27489).

1. Koshland, D. E., Jr. (1970) in *The Enzymes*, ed. Boyer, P. D. (Academic, New York), 3rd Ed., Vol. 1, pp. 342–397.
2. Eigen, M. (1974) in *Quantum Statistical Mechanics in the Natural Sciences*, eds. Mintz, S. L. & Wiedermeyer, S. M. (Plenum, New York), pp. 37–61.
3. Hammes, G. G. & Wu, C-W. (1974) *Annu. Rev. Biophys. Bioeng.* **3,** 1–34.
4. Weber, G. (1972) *Biochemistry* **11,** 864–878.
5. Lakowicz, J. R. & Weber, G. (1973) *Biochemistry* **12,** 4171–4179.
6. McCammon, J. A., Gelin, B. R. & Karplus, M. (1977) *Nature (London)* **267,** 585–590.
7. Yguerabide, J., Epstein, H. F. & Stryer, L. (1970) *J. Mol. Biol.* **51,** 573–590.
8. Lovejoy, C., Holowka, D. A. & Cathou, R. E. (1977) *Biochemistry* **16,** 3668–3672.
9. Mendelsohn, R. A., Morales, M. F. & Botts, J. (1973) *Biochemistry* **12,** 2250–2255.
10. Lopez-Delgado, R., Tramer, A. & Munro, I. H. (1976) *Chem. Phys.* **5,** 72–82.
11. Bénard, C. & Rousseau, M. (1974) *J. Opt. Soc. Am.* **64,** 1433–1444.
12. Brown, J. R. (1976) *Fed. Proc. Fed. Am. Soc. Exp. Biol.* **35,** 2141–2144.
13. Davis, A., Moore, I. B., Parker, D. S. & Taniuchi, H. (1977) *J. Biol. Chem.* **252,** 6544–6553.
14. Eylar, E. H., Brostoff, S., Hashim, G., Caccam, J. & Burnett, P. (1971) *J. Biol. Chem.* **246,** 5770–5786.
15. Ambler, R. P. (1971) in *Recent Developments in the Chemical Study of Protein Structure*, eds. Previers, A. J.-F. & Collette-Previers, M.-A. (Institut National de la Santé et de la Recherche Médicale, Paris), pp. 239–289.
16. Yguerabide, J. (1972) *Methods Enzymol.* **26,** 498–578.
17. Wahl, P. (1975) *New Tech. Biophys. Cell Biol.* **2,** 233–241.
18. Belford, G. G., Belford, R. L. & Weber, G. (1972) *Proc. Natl. Acad. Sci. USA* **69,** 1392–1393.
19. Gottlieb, Y. Y. & Wahl, P. (1963) *J. Chim. Phys.* **60,** 849–856.
20. Kinosita, K., Jr., Kawato, S. & Ikegami, A. (1977) *Biophys. J.* **20,** 289–305.
21. Dale, R. D. & Eisinger, J. (1974) *Biopolymers* **13,** 1573–1605.
22. Marquardt, D. W. (1963) *J. Soc. Ind. Appl. Math* **11,** 431–441.
23. Bevington, P. R. (1969) *Data Reduction and Error Analysis for the Physical Sciences* (McGraw-Hill, New York), pp. 235–240.
24. Grinvald, A. & Steinberg, I. Z. (1974) *Anal. Biochem.* **59,** 583–598.
25. Grinvald, A. (1976) *Anal. Biochem.* **75,** 260–280.
26. Hodgson, K. O., Winick, H. & Chu, G. (1976) *Stanford Synchrotron Radiation Laboratory Report 76/100,* Synchrotron Radiation Research (Stanford Univ., Stanford, CA).
27. Veatch, W. R. & Stryer, L. (1977) *J. Mol. Biol.* **117,** 1109–1113.
28. Rosen, P. & Pecht, I. (1976) *Biochemistry* **15,** 775–786.
29. Grinvald, A., Schlessinger, J., Pecht, I. & Steinberg, I. Z. (1975) *Biochemistry* **14,** 1921–1929.
30. Hirschfeld, H., Teitelbaum, D., Arnon, R. & Sela, M. (1970) *FEBS Lett.* **7,** 317–320.
31. Weber, G. (1960) *Biochem. J.* **75,** 335–345.
32. Weber, G. (1960) *Biochem. J.* **75,** 345–352.
33. Shapiro, S. L., ed. (1977) *Ultrashort Light Pulses: Picosecond Techniques and Applications* (Springer, New York).
34. Cotton, F. A., Bier, D. J., Day, V. W., Hazen, E. E., Jr. & Larsen, S. (1972) *Cold Spring Harbor Symp. Quant. Biol.* **36,** 243–249.
35. Eylar, E. H. & Thompson, M. (1969) *Arch. Biochem. Biophys.* **129,** 468–479.
36. Krigbaum, W. R. & Hsu, T. S. (1975) *Biochemistry* **14,** 2542–2546.
37. Eylar, E. H., Caccam, J., Jackson, J., Westall, F. & Robinson, A. (1970) *Science* **168,** 1220–1223.
38. Finnazi-Agro, A., Rotilio, G., Avigliano, L., Guerrieri, P., Boffi, V. & Mondovi, B. (1970) *Biochemistry* **9,** 2009–2014.
39. Adman, E. T., Stenkamp, R. E., Sieker, L. C. & Jensen, L. H. (1978) *J. Mol. Biol.* **123,** 35–47.
40. Visscher, R. B. & Gurd, F. R. N. (1975) *J. Biol. Chem.* **250,** 2238–2242.
41. Wüthrich, K. & Wagner, G. (1975) *FEBS Lett.* **50,** 265–268.
42. Hull, W. E., & Sykes, B. D. (1975) *J. Mol. Biol.* **98,** 121–153.
43. Snyder, G. H., Rowan, R., III, Karplus, S. & Sykes, B. D. (1975) *Biochemistry* **14,** 3765–3777.
44. Hetzel, R., Wuthrich, K., Deisenhofer, J. & Huber, R. (1976) *Biophys. Struct. Mech.* **2,** 159–180.